Journal of Environmental & Earth Sciences
https://journals.bilpubgroup.com/index.php/jees

ARTICLE

Spatiotemporal Variation and Driving Analysis of Net Primary Productivity of Vegetation in Southern Part of Taihang Mountain, China

Taiyi Cai [1], *ChengLong He* [2], *Ammara Gill* [2], *Chao Ma* [2,3,4*]

[1] *Institute of Quantitative Remote Sensing & Smart Agriculture, Henan Polytechnic University, Jiaozuo 454003, China*

[2] *School of Surveying and Land Information Engineering, Henan Polytechnic University, Jiaozuo 454003, China*

[3] *Key Laboratory of Spatio-Temporal Information and Ecological Restoration of Mines (MNR), Henan Polytechnic University, Jiaozuo 454003, China*

[4] *Research Centre of Arable Land Protection and Urban-Rural High-Quality Development in Yellow River Basin, Henan Polytechnic University, Jiaozuo 454003, China*

ABSTRACT

The net primary productivity of vegetation (NPP) is an important index to evaluate the carbon sequestration capacity of vegetation and land use change. Using MOD17N3HGF NPP data, climate data and night-time light data from 2000 to 2020, this study explored the relationship between NPP and urban expansion, land use and climate change in the Southern Part of Taihang Mountain through brightness gradient method, trend analysis, partial correlation analysis and contribution analysis. It aims to provide information support for urban and rural planning and ecological management in this region. Key findings include: Over the past 20 years, NPP in mountain areas has shown an overall fluctuating upward trend, with an "N" pattern related to altitude. The human activity area expanded by 9.9%, with expansion of highly active areas holding back NPP growth and moderately active areas contributing to it. The trend of climate change is gradually warming and wetting, and the correlation between precipitation and NPP is strong, while the correlation between temperature and NPP is weak. Compared with human activities (19.9%), precipitation was the main driver of NPP change, contributing significantly up to

*CORRESPONDING AUTHOR:
Chao Ma, School of Surveying and Land Information Engineering, Henan Polytechnic University, Jiaozuo 454003, China; Key Laboratory of Spatio-Temporal Information and Ecological Restoration of Mines (MNR), Henan Polytechnic University, Jiaozuo 454003, China; Research Centre of Arable Land Protection and Urban-Rural High-Quality Development in Yellow River Basin, Henan Polytechnic University, Jiaozuo 454003, China; Email: mac@hpu.edu.cne

ARTICLE INFO
Received: 26 August 2024 | Revised: 20 October 2024 | Accepted: 28 October 2024 | Published Online: 14 January 2025
DOI: https://doi.org/10.30564/jees.v7i1.7137

CITATION
Cai, T., He, C,, Gill, A., et al., 2025. Spatiotemporal Variation and Driving Analysis of Net Primary Productivity of Vegetation in Southern Part of Taihang Mountain, China. Journal of Environmental & Earth Sciences. 7(1): 611–624. DOI: https://doi.org/10.30564/jees.v7i1.7137

79.5%. In the past 20 years, the ecological quality of the south Taihang Mountain region has improved significantly and actively responded to climate change, but human activities have led to spatial and temporal ecological differences.
Keywords: Climate Change; MODIS NPP; Man-Land Relationship; Southern Part of Taihang Mountain

1. Introduction

Net Primary Productivity (NPP) is the total organic matter produced by vegetation through photosynthesis per unit time and per unit area, minus the amount used for respiration [1]. It plays an important role in the material and energy cycles of the ecosystem and is one of the key indicators for measuring the productivity of plant communities [2, 3]. Changes in NPP are mainly influenced by human activities and climate change [4]. Human activities such as urban expansion, resource exploitation, and pollutant emissions caused by environmental degradation, combined with environmental protection measures such as farmland restoration, reforestation, urban greening and mine reclamation aim to counteract these negative impacts. In addition, climate change has led to global temperature rise and changes in precipitation patterns, which have also led to regional water resource imbalance [5]. Today's environmental challenges are complex and urgent. A timely and accurate understanding of NPP changes under natural and anthropogenic influences is crucial for effective environmental management, sustainable resource use and urban planning.

Given the rigorous mathematical and physical modeling of NPP and their robustness as indicators of ecological quality for monitoring, numerous studies have been conducted in recent years to investigate the response of NPP to human activities and climate change. It is important to note that the nature and magnitude of the influence of external factors on NPP changes varies considerably between regions and ecological environments. During 2001–2020, precipitation below 2300 m above sea level has a greater effect on NPP than temperature in the Yangtze River Basin, while above 2300 m, on the contrary, human activities promote the overall increase of NPP [6]. From 2000 to 2020, temperature was negatively correlated with NPP in most parts of the Yellow River Basin, while local precipitation showed a positive correlation. The increase in NPP was facilitated by farmland restoration, afforestation, and tree planting initiatives [7]. In the middle and upper reaches of the Yellow River from 2000 to 2015, the fragmentation degree of forest, grassland, and shrub types increased, and the aggregation degree decreased under the strong human disturbance. Different dominant landscape types resulted in strong spatial heterogeneity of NPP distribution, but the total NPP of each type showed an increasing trend [8]. From 2000 to 2020, NPP in the central Tianshan Mountains shows an upward trend. The conversion of grassland and oasis into building land leads to the expansion of the urban area, and the desertification of cultivated land and building land is the main factor for the increase in NPP [9]. Between 1982 and 2015, the NPP in the Qinling Mountains was more affected by precipitation, showing a distinct seasonality under the conditions of climate change and warming [10]. From 2001 to 2018, both temperature and precipitation contributed to the increase in NPP in southwest China, but temperature had a larger effect [11]. From 1982 to 2015, China's overall NPP shows an increasing trend, and the NPP of urban land in the Beijing-Tianjin-Hebei city cluster, the Yangtze River Delta city cluster, and the Pearl River Delta city cluster shows a decreasing trend, while the buffer zone shows an increasing trend. The effect of temperature and sunshine on NPP is positive, but the effect of vegetation reduction is not significant [12]. From 2000 to 2015, most forest NPP in Nepal exhibited an increasing trend, with the highest rates observed in the plains, followed by hills, and the lowest in the mountains. The interannual NPP variation trend correlated with climate patterns [4]. Between 2001 and 2015, southern Iran experienced a significant increase in temperature, while precipitation changes were not significant. Precipitation played a key role in the changes in NPP, which are projected to continue to increase in the future [13]. From 2009 to 2019, evapotranspiration and temperature increased in Tanzania, while precipitation decreased, and NPP was significantly positively correlated with precipitation and evapotranspiration, and NPP will increase in the future except in the southwestern region of the country [14]. In addition, night-time light (NTL), as an objective remote sensing index, is closely related to population density, economic activities, and energy consumption, and can comprehensively characterize the degree of impact and development trends of human activities. It is widely used as the most important data source for monitoring human activity and land use intensity on a regional scale, as well as for studying changes in urban distribution and patterns [15, 16], and for assessing levels of economic development and social activity [15, 17].

Overall, most of the existing research has focused on the spatio-temporal variability of NPP and its response to human activities, climate change, and other factors. However, several problems and deficiencies were identified in the literature: (1) The multi-factorial interactions between human activities and climate change at scales below the county and municipal levels have not received sufficient attention. (2) Most existing studies use land use type changes as a basis for human activity, and the use of NTL, which can directly reflect human social and economic activities, is limited. (3) Quantitative studies of the contribution of human activities and climate change toNPP are inadequate, and the extent of multi-factorial effects is rarely assessed.

Taking some cities in the southern part of Taihang Mountain as examples, this study used night light data, land use data, NPP and climate data to study the complex response of human activities and climate change to NPP. The main contributions of this paper are as follows: (1) To study the changes of NPP in the South Taihang region, to timely understand the impact of global warming on nationally important ecological functional areas, and to provide remote sensing technology support to ensure the safety of the carbon pool in the South Taihang region. (2) To study the NPP variation characteristics and influencing factors in the agricultural area of the southern foot of Taihang Mountain, and to make remote sensing contributions to ensuring food security and promoting sustainable agriculture in the region. (3) To monitor the NPP changes in the Taihang Mountain area and obtain the ecological changes of important water sources in northern Henan, so as to ensure the safe, and sustainable development of water resources in northern Henan. (4) The study includes land use and NPP changes in Yuntaishan National Nature Reserve and Taihang Macaque Nature Reserve, which can provide technical support for the protection, restoration, sustainable development and biodiversity conservation of terrestrial ecosystems. (5) The characteristics of urban expansion in South Taihang and its impact on NPP were studied to provide data guarantee for the construction of a safe and healthy living environment. The study is of great significance for an in-depth understanding of the impact of human activities and climate interaction on the ecosystem and formulating sustainable development strategies, and the results will provide a scientific basis and reference for regional environmental protection and ecological restoration.

2. Overview of the Study Area

Situated at the geographical boundary between the second and third terrains of the Chinese landscape and the watershed separating the North China Plain from the Loess Plateau, the Taihang Mountains play a critical role as an important ecological barrier in the central region of China. Thanks to South Taihang's rich mineral resources and high-quality tourism conditions, cities in South Taihang have large-scale and relatively developed economic conditions.

The study area includes several cities close to South Taihang and Northern Henan, namely Jiyuan, Qinyang, Boai, Jiaozuo, Xiuwu, and Huixian. The geographical coordinates of the area are between 34°53′ and 35°50′ N latitude and 112°1′ and 113°56′ E longitude. With a total area of approximately 5786 km^2, the region exhibits altitudes ranging from 72 m to 1923 m. The average altitude is measured at 346.7 m. The landforms within the study area consist of plains, hills, and mountains, accounting for 43.8%, 18.4% and 37.8% of the total area, respectively (**Figure 1**).

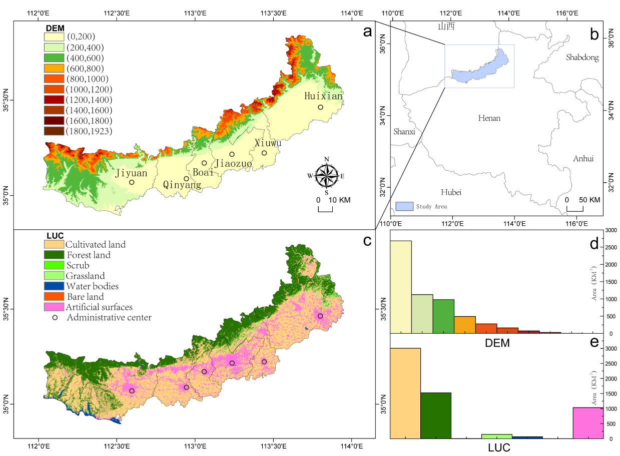

Figure 1. Overview of the study area.

The northern part of the study area consists of South Taihang, which features rugged terrain and extends from northeast to southwest. Notable features in this area include the Yuntai Mountain National Nature Reserve, the Taihang

Mountain Macaque Nature Reserve, and several tourist attractions rated 4A or above. On the other hand, the southern plain exhibits a vast expanse and is endowed with well-developed water systems, encompassing major rivers, for instance the Yellow River, Qinhe River, and Dashahe River. The region has high quality arable land and favorable irrigation conditions for agricultural production, with winter wheat, summer corn and other crops being the primary focus. The climate is classified as a temperate continental monsoon climate, with an average annual precipitation ranging from 564.9 mm to 736.5 mm and an average annual temperature ranging from 8.5 °C to 15.6 °C.

3. Materials and Methods

3.1. Data Acquisition and Processing

Key data used in this study include:
(1) The NPP data were obtained from the MOD17A3HGF (2000–2020) dataset provided by the US National Aeronautics and Space Administration (NASA), available at (https://ladsweb.modaps.eosdis.nasa.gov/). This dataset is derived from MODIS/TERRA satellite remote sensing data and uses the BIOME-BGC model to estimate NPP. The spatial resolution of the dataset is 500 m and the temporal resolution is annual. Data extraction was performed using the MODIS Reprojection Tools (MRT) software. (2) The climatological data utilized in this study were obtained from the National Tibetan Plateau Data Center (https://data.tpdc.ac.cn/)[18, 19]. These data include the China 1-km monthly mean temperature dataset (1901–2022) and the China 1-km monthly precipitation dataset (1901–2022). The generation of these two datasets involved the application of the Delta downscaling scheme by Peng Shouzhang, using the global climate dataset published by CRU and WorldClim specifically for China. The temperature data are provided in units of 0.1 °C, while the precipitation data are reported in units of 0.1 mm. The spatial resolution of both datasets is approximately 1 km. MATLAB software was employed for data extraction and conversion into TIFF format. The annual total precipitation was derived from the monthly precipitation data, and the monthly average temperature was aggregated to obtain the annual average temperature. (3) A Prolonged Artificial Night-Time Light Dataset of China (PANDA) utilized in this study was obtained from the National Tibetan Plateau Scientific Data Center (https://data.tpdc.ac.cn/)[20]. It was calculated and published by Zhang Lixian et al., employing the Night-Time Light Convolutional Long Short-Term Memory (NTLSTM) network method. This approach was based on the existing night-time light data from VIIRS and DMSP sources. The dataset has a spatial resolution of approximately 1 km and a temporal resolution of 1 year. (4) The China Land Cover Dataset (CLCD) utilized in this study was developed by Jie Yang et al. (30 m annual land cover and its dynamics in China from 1990 to 2019 - Zenodo). It was created by analyzing a vast collection of remote sensing images available on the Google Earth Engine platform. The classification process involved the use of a random forest classifier to assign land cover categories[21]. The CLCD includes various land cover types such as cultivated land, forest land, scrub, grassland, water bodies, ice and snow, bare land, artificial surfaces, and wetlands. (5) The elevation data used in this study are obtained from the NASA Space Shuttle Radar Topographic Mission (SRTM) dataset. The SRTM dataset creates a digital elevation model by measuring the Earth's surface altitude using radar equipment aboard the US Space Shuttle Endeavour. The SRTM digital elevation model has a spatial resolution of 30 meters.

Finally, MODIS NPP data, climate data, and night light data are resampled to obtain a consistent spatial resolution of 1 km. The sampling method is the nearest neighbor method. All data were projected using the UTM WGS84 49N projection.

3.2. Methods

3.2.1. Human Activity Level Extraction Based on NTL

Based on the PANDA dataset, NTL was graded using Brightness Gradient (BG) to indicate the intensity of human activities[22]. At the local scale, there is a quadratic relationship between NTL and the corresponding BG, which describes the pixel-level variation in luminance in the area of human activity. BG is defined as the maximum rate of change of the NTL value from the center pixel to the adjacent pixel within a given range. To eliminate the influence of anomalous pixels on the result, the BG of each raster is calculated using the maximum mean method. The formula is:

$$BG = \sqrt{\frac{dNTL}{dx^2} + \frac{dNTL}{dy^2}} \tag{1}$$

$$dNTL/dx^2 = [(NTL_2 + NTL_5 + NTL_8) - (NTL_0 + NTL_3 + NTL_6)]/(8 \times pixelsize) \quad (2)$$

$$dNTL/dy^2 = [(NTL_6 + NTL_7 + NTL_8) - (NTL_0 + NTL_1 + NTL_2)]/(8 \times pixelsize) \quad (3)$$

Number the central pixel and the eight adjacent pixels from NTL_0 NTL_8 from left to right and from top to bottom. The BG from the central pixel to all adjacent pixels is estimated by the rate of change $dNTL/dx^2$ in the horizontal direction and the rate of change $dNTL/dy^2$ in the vertical direction. Quadratic polynomial fit of NTL and BG:

$$BG = aNTL^2 + bNTL + c \quad (4)$$

Where a, b and c are the coefficients of the fit polynomial.

The part with a high BG value generally appears in the area with a large NTL brightness change, that is, the transition area between urban and rural areas or the transition area between rural and undeveloped areas. The NTL data from 2000 to 2020 were processed by gradient. According to BG, the intensity of human activity was divided into three categories: high activity, medium activity, and low activity. The formula for calculating the split point is shown in **Table 1**:

Table 1. NTL-based human activity intensity segmentation point calculation.

Area	Partition Point	NTL	BG
Low activity region	$P_0(DN_0, BG_0)$	DN_{min}	$aDN_{min}{}^2 + bDN_{min} + c$
	$P_1(DN_1, BG_1)$	$-\frac{b}{2a} - \sqrt{\frac{BG_1 - C}{2a} + \frac{b^2}{4a^2}}$	$\frac{BG_0 + BG_2}{2}$
Medium activity region			
	$P_2(DN_2, BG_2)$	$-\frac{b}{2a}$	$x = \frac{4ac - b^2}{4a}$
High activity region	$P_3(DN_3, BG_3)$	DN_{max}	$aDN_{max}{}^2 + bDN_{max} + c$

3.2.2. Trend Analysis of the NPP

NPP data, climate data and lighting data are analyzed based on the unitary linear regression analysis method. In a linear regression model, the regression coefficient (slope) reflects the rate of change of the data, that is, the annual change of the data [23]. The formula is:

$$slope = \frac{n\sum_{i=1}^{n} i \times X_i - n\sum_{i=1}^{n} i \sum_{i=1}^{n} X_i}{n \times \sum_{i=1}^{n} i^2 - \left(\sum_{i=1}^{n} i\right)^2} \quad (5)$$

Where slope is the rate of change of the data, i is year I among all survey years n (n = 21), and X is the type of data to be examined. If slope > 0, it means that the data show an increasing trend; otherwise, it means that the data show a decreasing trend.

The significance of the changes in the data was verified using the F-test method (mainly for NPP data). This method is only used to evaluate the reliability of data trend changes, independent of the rate of data change. The formula is:

$$F = \frac{\sum_{i=1}^{n} (\widehat{y}_i - \bar{y})}{\sum_{i=1}^{n} (y_i - \widehat{y}) / (n-2)} \sim F(1, n-2) \quad (6)$$

Where $\widehat{y}_i$ is the regression value, $\bar{y}$ is the average of the data and n is the total number of years 21. According to the F-distribution criticality table, the trend of change can be divided into the following five classes: no significant change (p > 0.5), significant increase (slope > 0, 0.01 < p < 0.05), significant deterioration (slope < 0, 0.01 < p < 0.05), extremely significant increase (slope > 0, p < 0.01), extremely significant deterioration (slope < 0, p < 0.01).

3.2.3. Partial Correlation Analysis of NPP and Climate Factors

Based on a first-order partial correlation analysis, the influence of one variable of the climatic factors on NPP is studied while controlling for the other variable. First, the simple correlation coefficients between the two variables and NPP are calculated and the formula is as follows:

$$R_{xy} = \frac{\sum_{i=1}^{n} \left[\left(x_i - \bar{x}\right) \left(y_i - \bar{y}\right) \right]}{\sqrt{\sum_{i=1}^{n} \left(x_i - \bar{x}\right)^2 \sum_{i=1}^{n} \left(y_i - \bar{y}\right)^2}} \quad (7)$$

Where R_{xy} is the simple correlation coefficient between climate factors and NPP, x_i and y_i are the values of climate factors and NPP in year i, $\bar{x}$ and $\bar{y}$ are the average values of climate factors and NPP, and n is the total number of years.

Then the partial correlation coefficient of the first order is obtained and the formula is as follows:

$$r_{x_1y\cdot x_2} = \frac{r_{x_1y} - r_{x_2y}r_{x_1x_2}}{\sqrt{1-r_{x_2y}^2}\sqrt{1-r_{x_1x_2}^2}} \tag{8}$$

Where $r_{x_1y\cdot x_2}$ represents the partial correlation coefficient between climate factor x_1 and NPP, holding climate factor x_2 constant. r_{x_1y}, r_{x_2y}, and $r_{x_1x_2}$ represent the simple correlation coefficients between climate factor x_1 and NPP, between climate factor x_2 and NPP and between the two climate factors.

3.2.4. Contribution Analysis

The contribution value was obtained by multiplying the rate of change of each influence factor by the weight of its influence on NPP, and the contribution of each influence factor to the long-term trend in vegetation NPP was studied [24, 25]. The formula is as follows:

$$K_{npp} = C_{pre} + C_{tmp} + C_{ntl} \tag{9}$$

$$C_{pre} = \frac{\alpha_{npp}}{\alpha_{pre}} * K_{pre} \tag{10}$$

Where K is the rate of change and C is the contribution value. $\frac{\alpha_{npp}}{\alpha_{pre}}$ is the partial derivative of the multiple regression of NPP on various influencing factors, representing the weight of pre in the factors influencing NPP. When multiplied by the rate of change of pre K_{pre}, the contribution value of pre to the change of NPP is C_{pre}.

$$P_{pre} = \frac{C_{pre}}{C_{pre} + C_{tmp} + C_{ntl}} \tag{11}$$

In order to integrate the regions with large differences in the contribution value of each factor to NPP, the influence weight of each factor to NPP is represented in the form of contribution degree P. The objective of this study was to analyze the relative influence of temperature, precipitation, and human activities on changes in NPP. To achieve this, we focused solely on these factors in our calculations, disregarding other potential influences.

4. Results

4.1. Spatial and Temporal Patterns of the NPP

The average NPP for the period 2000–2020 shows variations between 230.23 and 382.68 gC m^{-2}, with a multi-year average of 307.62 gC m^{-2}. As shown in **Figure 2a**, the lowest average NPP was observed in 2001, while the highest occurred in 2020, with a range of 152.45 gC m^{-2}. The NPP in the study area shows a fluctuating increasing trend, with an average increasing trend of 3.89 gC m^{-2} a^{-1}, p = 0.6054. Out of the 21 years analysed, the mean NPP was lower than the multi-year mean NPP in 11 years, especially in the period 2000–2010. In particular, the NPP was particularly high in 2003 and 2004, followed by a fluctuation below the mean line, after which it returned to normal levels in 2005. From 2015 onwards, only 2019 showed a lower NPP value compared to the mean.

The distribution of mean NPP at different altitudes is depicted in **Figure 2b**. NPP shows a gradient distribution pattern with increasing altitude. Initially, it first reaches the lowest value of 254.76 gC m^{-2} from the plain area to 200 m. Subsequently, NPP increases rapidly from 200 m and reaches its maximum value of 352.46 gC m^{-2} between 400 and 600 m. However, there is a sharp decrease at 600 m, followed by another decrease after leveling off at 900–1200 m. At 1400–1500 m, NPP reaches its lowest value of 177.02 gC m^{-2} before rising sharply to its maximum value at the southern part of Taihang Mountain boundary. The trend of NPP increasing rate with altitude mirrors that of NPP distribution, with average increasing trend ranging from 0.63 to 6.21 gC m^{-2} a^{-1}).

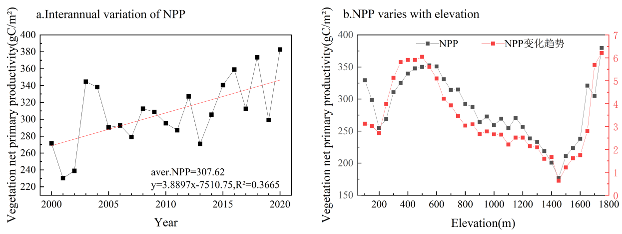

Figure 2. (**a**) Interannual variation of NPP and (**b**) its relationship with elevation.

Figure 3 illustrates that across the study area, the majority of pixel NPP falls within the range of 200–500 gC m^{-2}. During 2000–2020, the number of pixels of 200–400 gC m^{-2} decreased significantly, while the number of pixels of 400–500 gC m^{-2} increased significantly, especially after 2013. About 8.5% of the pixel NPP is consistently below 100 gC m^{-2}, and these areas are mainly distributed in plain areas. About 5.6% of the pixel NPP remained between 100 and 200 gC m^{-2}, and these regions were mainly located at higher elevations in mountainous areas. Specifically, in 2002, the ecological quality was the worst, with 23.5% of pixel NPP below 200 gC m^{-2}, and 76.5% of pixel NPP between 200–400 gC m^{-2}. In contrast, 2020 has the best ecological quality, with 62% of pixels having NPP higher than 400gC m^{-2}.

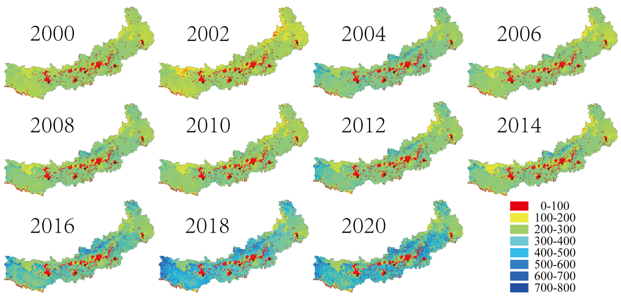

Figure 3. Spatial distribution of NPP from 2000 to 2020.

4.2. Changing Characteristics of Human Activities

The results of brightness gradient extraction show that there is an expanding range of volatility in the evolution of different active regions in the past 21 years (**Figure 4**). The areas with high activity levels are mainly concentrated in Huixian, Jiaozuo and Jiyuan. The areas with high activity levels are mainly concentrated in Huixian, Jiaozuo and Jiyuan. The evolution of human activity patterns is characterized by the transition from medium to high activity areas in the plain at a rate of 9.51 km^2 per year. There is also an expansion of medium active region into low activity region in mountainous regions at a rate of 10.86 km^2 per year. The expansion of medium active region is mainly observed in Huixian and the northeast of Jiyuan, with the northern expansion limited by the Taihang Mountains. The high activity region, expanding region, and mid-level active region are mainly located in the plain areas, with average elevations of 129 m, 134.7 m, and 188 m, respectively. On the other hand, the expansion region of the medium active region is mainly observed in the hilly areas, characterized by an average altitude of 520 m. The low activity areas are mainly distributed in mountainous regions with an average altitude of 837.9 m.

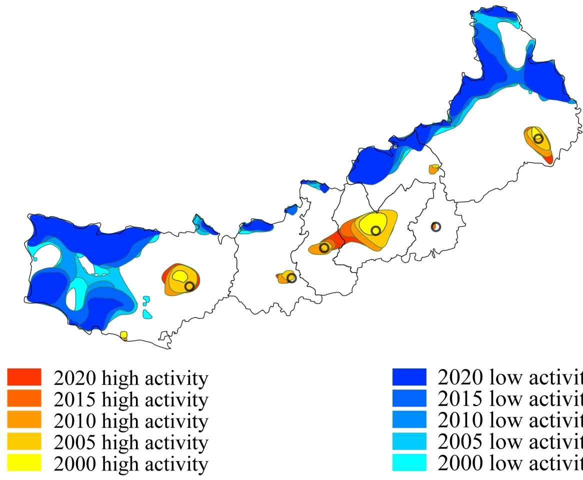

Figure 4. Changes in human activity levels and coverage.

Table 2 shows the observed changes in land use. Over the last 21 years, there has been a significant decrease in cultivated land and grassland, connected with a significant increase in water bodies and artificial surfaces. Specifically, the area of cultivated land has decreased by almost 7%, while the area of grassland has decreased by 136.28 km^2. On the other hand, water bodies have increased by 36.3 km^2 and artificial surfaces by a significant 334.79 km^2. The woodland area, however, has changed only slightly. Comparing the land use in the subdistrict between 2000 and 2020, the following changes have occurred.

Table 1. Type of land use (unit: km^2).

Type	Year				
	2000	2005	2010	2015	2020
Cultivated land	3233.06	3182.13	2972.08	2974.93	3005.70
Forest land	1527.58	1511.46	1625.64	1509.59	1527.31
Scrub	14.65	16.51	13.36	13.86	7.44
Grassland	282.00	261.11	247.76	250.45	145.72
Water bodies	29.04	48.78	56.92	63.26	65.34
Bare land	0.03	0.03	0.18	0.06	0.05
Artificial surface	699.65	765.98	870.06	973.86	1034.44

The high activity region is mainly characterized by artificial surfaces, which increased from 77.0% in 2000 to 93.1% in 2020. The share of cultivated land decreased from 22.6% to 6.6%. The expansion zone of the high activity region has shifted from predominantly cultivated land to primarily consisting of artificial surfaces. Cultivated land has decreased from 70.2% to 43.6%, while the area occupied by artificial surfaces has increased from 29.1% to 55.1%. The medium active region is mainly composed of arable land, with artificial surfaces in second place. Arable land has decreased from 74.7% to 70.2%; however, the area of artificial surfaces has increased from 14.6% to 21.0%. The expansion region of the medium active area has mainly affected forest and cultivated land, resulting in minimal changes. The area of cultivated land has increased from 37.1% to 39.2%, while the area of forest land has increased from 48.5% to 49.2%, and the area of grassland has decreased from 9.8% to 5.5%. The low activity region is mainly characterized by forest land, followed by cultivated land. The forest area has increased from 84.9% to 85.8%, while the cultivated area has increased from 8.1% to 9.0%. The area of grassland decreased from 5.6% to 3.5%.

4.3. Impact of Climate on Changes in NPP

The overall climate change in the study area from 2000 to 2020 is shown in **Figure 5a,b**. (1) The annual precipitation showed a fluctuating and gradually increasing trend, with a growth rate of 0.97 mm a^{-1}. From 2000 to 2004, the minimum value was 423.5 mm in 2001, while the maximum value was 860.9 mm in 2003, with a range of 437.4 mm. Subsequently, from 2004 to 2011, the precipitation level was relatively stable, along with small fluctuations in the following period. (2) The annual average temperature in the study area showed a fluctuating upward trend, with a growth rate of 0.01 °C a^{-1}. Over the period from 2000 to 2020, the temperature variations were minimal and evenly distributed, with the lowest value of 13.8 °C in 2003 and the highest value of 14.9 °C in 2006.

The spatial distribution of mean annual precipitation and temperature is shown in **Figure 6a** and **Figure 6b**, respectively. Due to the altitude factor, the distribution of precipitation and temperature is very different. The difference between the maximum and minimum values is 171.5 mm for precipitation and 7.1 °C for temperature, respectively. The spatial distribution of both factors shares similarities, with high precipitation and low temperature in the mountainous regions and low precipitation and high temperature in the plains. The elevation of the plain remains relatively consistent, but there are several small areas of anomalous temperature and precipitation, and these areas display slightly high values in both precipitation and temperature compared to the surrounding regions.

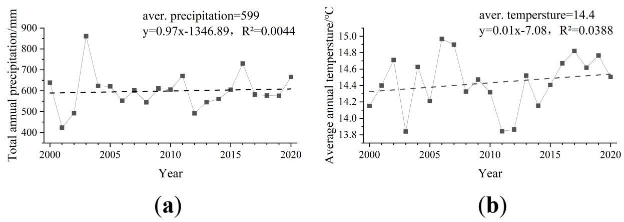

Figure 5. Interannual variation of (**a**) precipitation and (**b**) temperature.

On a zonal scale, climate differences are shown in **Figure 6**. The lowest average temperature was 12.3 °C in the low active region, and the average temperature gradually increased from the low active region to the high active region, with the highest temperature being 15.4 °C. Annual precipitation is highest in the low active area and lowest in the medium active area. The precipitation in descending order was low active region (643.8 mm), expansion region of the medium active region (612.9 mm), high active region (600.3 mm), expansion region of the high activity region (586.4 mm), and medium active region (584.3 mm).

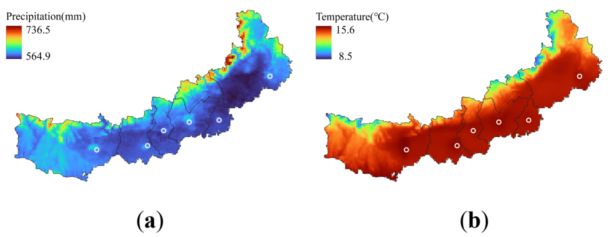

Figure 6. Spatial distribution of climate factors: (**a**) precipitation and (**b**) temperature.

4.4. Impact of Human Activity on Changes in NPP

The variation of NPP among different active regions differs significantly. The mean NPP values of the medium active region and the expanding region were similar and higher than those of the low active region. The average NPP in the medium active region was slightly higher than that in the expansion region of the medium active region (324.46 gC m^{-2} > 323.37 gC m^{-2}). The average NPP of the expansion region of the high active region were much higher than that of the high active region (235.62 gC m^{-2} > 58.67 gC m^{-2}), but still lower than the levels in all regions.

The spatial distribution of NPP changes is shown in **Figure 7**. The average NPP of all regions increased at different rates between 2000 and 2020, and the proportion of pixels in a region shows an increasing trend, which determines the rate of growth. In the medium active region and the expansion region, the NPP of more than 73% of the pixels significantly increased. Only 1.2% of the pixels in the whole region showed a deteriorating trend, mainly distributed in the high and medium active regions. Pixels with no significant change accounted for 33.9% of the total study area, 85.9% of the high active region and 69.3% of the low active region. The NPP of 66.3% of the pixels in the expansion region of the high activity region showed no obvious change or degradation trend. Over the last 21 years, the NPP of most pixels in the high and low active regions remained stable or did not change significantly. The NPP of most pixels in the medium active region and the expansion region increased significantly.

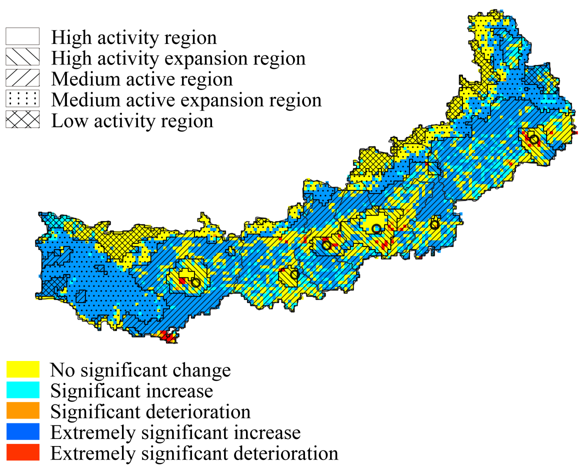

Figure 7. NPP trend overlaid with active regions.

The correlation analysis of average NTL and average NPP in the region showed that NTL and NPP in the highly active region exhibited a low negative correlation ($r = –0.1923$, $p = 0.4035$). There was a low positive correlation between NTL and NPP in the expansion region of the high activity region ($r = 0.2237$, $p = 0.3294$). There was a significant positive correlation between NTL and NPP in the medium activity region and its expanding region, and the correlation and significance in the medium activity region's expanding region ($r = 0.4805$, $p = 0.0274$) were slightly stronger than those in the medium activity region ($r = 0.4033$, $p = 0.0698$). There was little correlation between NTL and NPP in low active regions ($r = 0.1002$, $p = 0.6655$).

From 2000 to 2020, both the highly and medium active regions expanded in a large area. In the process of expansion of highly active region, the number of degraded pixels increased. Simultaneously, the average increasing rate of NPP decreased, despite this the artificial surface expansion did not cause large-scale damage to vegetation. Thus, NTL did not show a significant negative correlation with NPP. The NPP in the medium active region and the expansion region showed a significant increase over a large range, and the average increasing trend was higher.

4.5. Impact of Climate on Changes in NPP

In general, NPP was highly correlated with precipitation ($r =0.5506$, $p = 0.0119$) but poorly correlated with air temperature ($r = 0.1271$, $p = 0.5933$). There is a significant positive correlation between annual precipitation and NPP in all regions. The low active region was the strongest ($r = 0.6448$, $p = 0.0021$), and the high active region was the weakest ($r = 0.4123$, $p = 0.0708$). The medium active region ($r = 0.5317$, $p = 0.0158$) was stronger than the expansion region of the medium active region ($r = 0.4815$, $p = 0.0316$), and the expansion region of the high active region was stronger than that of the high active region ($r = 0.5428$, $p = 0.0134$). The correlation between NPP and mean annual temperature varied between regions. The correlation between NPP and temperature was weak in the high and low active regions ($r = 0.2680$, $p = 0.2533$ and $r = 0.2367$, $p = 0.3294$, respectively), and lowest in the low active region ($r = 0.1002$, $p = 0.6655$). However, in the medium active region and its expanding region, there was a significantly higher positive correlation. The correlation was even higher in the expanding region of the medium active region ($r = 0.4805$, $p = 0.0274$) than in the medium active region itself ($r = 0.4623$, $p = 0.0235$).

The spatial distribution is shown in **Figure 8**. In the entire study zone, 92.3% of pixel NPP was positively correlated with precipitation. 28.7% of the pixel NPP was negatively correlated with air temperature, and only 8.8% was positively correlated with higher NPP, mainly distributed in the southwest of Jiyuan and the plain. It is worth noting that in the regions with low human activity, the northern mountain area of the study area is affected by altitude, and pixel NPP generally has a strong positive correlation with precipitation, and a low or negative correlation with temperature. The southwest of Jiyuan is close to the Xiaolangdi reservoir, and the correlation between NPP and precipitation is lower, while the correlation between NPP and temperature is higher.

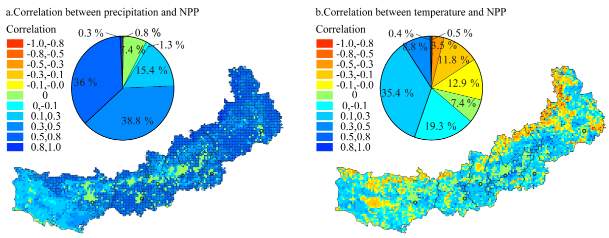

Figure 8. Correlation between climate factors and NPP.

Note: ●: $p < 0.01$; ■: $0.01 \leq p < 0.05$; ▲: $0.05 \leq p < 0.1$.

4.6. Analysis of Dominant Factors of NPP Change

Figure 9 shows the results of contribution analysis. Across the entire study region, precipitation emerged as the most influential factor, contributing to 79.4% of the variation in NPP, whereas air temperature played a negligible role, contributing less than 1%. Moreover, only a small fraction (5.6%) of pixels exhibited a temperature-related contribution exceeding 2%.

Human activity intensity exhibited varying impacts based on activity patterns, with the contributions of different factors to NPP changes showing significant regional discrepancies: (1) In the expanding region of the highly active area, human activities accounted for 47.4% of the NPP change, significantly higher than the 15.1% observed in the highly active area. This disparity underscores the greater influence of human activities during expansion processes. (2) Within the moderately active area, human activities contributed 22.9%, surpassing the 15.3% observed in the expanding segment of the same region. In contrast to the significant impact of expansion in highly active regions, the influence of expansion in moderately active regions on NPP was less pronounced. (3) The contribution of human activities gradually decreased from the expanding highly active region to the low activity region, while the influence of precipitation increased. In the low activity region, human activities made minimal contributions, with precipitation accounting for 98.7% of the overall influence on NPP.

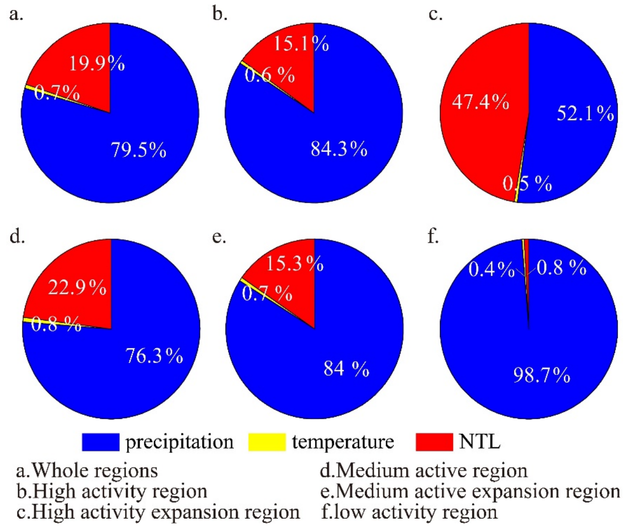

Figure 9. Pie chart of the contribution ratio of the three impact factors in each sub-region.

5. Discussion

In the southern region of Taihang Mountain, elevation, topographic factors, and human activities give rise to distinct vegetation conditions, thereby causing significant spatial heterogeneity in the distribution and change of NPP in this area. Against the backdrop of global climate change and intensifying human activities, the ecological quality assessment of the southern Taihang Mountains should be comprehensive. Human activities frequently lead to alterations in land use types, and diverse utilization modes will have varying influences on NPP changes [26]. Previous studies have quantitatively characterized the impacts and extent of human activities on the land surface through land use in various manners [27, 28]. Nevertheless, human factors such as population density and urban expansion also have an impact on ecological quality, which is also an embodiment of human activities. The numerical NTL can extract precise and reliable information on human activities on a large scale, analyze the long-term change trend of the scope and intensity of human activities and the distribution law along with the altitude terrain. Different brightness gradients represent the intensity of human activities, and the conversion ratio of land types under different intensities of human activities indirectly reflects the disparities in human production and lifestyles. The combination of long time series of PANDA with land use type data offers insights into the interaction between human activities and climate change on NPP changes.

In the plain or hilly regions south of Taihang Mountain, the intensity of human activities continues to increase, a small part of cultivated land is transformed into building land, the scope of built-up area gradually expands, and local vegetation is destroyed. But arable land still dominates. Human activities interfere with crops through irrigation to make crops grow within a certain limit without temperature restriction [29], and the progress of agricultural technology will also promote the significant growth of NPP in this region. Regions with ample water or developed agricultural activities have water sources other than precipitation, the demand for precipitation is lower, and higher temperatures also promote plant growth in these regions. In addition, the conversion of grassland to arable land or forest land is also the reason for the increase in NPP. In contrast, high-altitude mountain areas have more precipitation and lower temperature, but still have a very high dependence on precipitation. However, the relationship between temperature and NPP is not clear, and may even be negatively correlated, which indicates that water shortage in high-altitude areas where precipitation is the only water source restricts plants from coping with high temperature and thus limiting their growth. This confirms that NPP in most areas of northern Henan has a relatively high growth trend from 2000 to 2010, but there is a degradation trend in north Jiyuan and northeast Jiaozuo [30]. NDVI in northern Henan shows an overall growth trend from 2020 to 2019, but it is basically unchanged in the Taihang Mountain area [31]. Part of the forest area in Taihang Mountain is 850–1850 m above sea level. With the increase of sea level, the diversity and aggregation of plant species decrease [32]. Therefore, the ecosystem in the high-altitude area is extremely fragile. In the future, the NPP level in the high-altitude region should be worried, while the NPP in the water-sufficient region will continue to increase within a certain temperature range.

In recent years, the government has taken a series of environmental protection measures, including the reforestation of South Taihang, and the conversion of farmland back to forest and grassland, and the implementation of mine management practices has yielded positive outcomes, and the observable trend of NPP growth is obvious in the middle and lower mountainous regions. However, as human urbanization breaks through the terrain boundary [33], the urban scale expands and NPP is destroyed in some areas of plains and hills. Extreme temperatures and extreme precipitation caused by continued global warming will pose a great challenge to most of our cities [34], and action to protect the environment cannot be delayed. As a natural carbon reservoir, the Taihang Mountains have the ability to reduce atmospheric carbon dioxide concentration and mitigate global warming in the ecosystem. According to this study, although the NPP in the southern part of Taihang Mountain has improved since 2000, the damage to the NPP caused by continuous urban expansion is inevitable, and the trend of the mid-altitude forest region in addressing global warming appears less optimistic.

Limitations and shortcomings of this study include: (1) The geographical extent of the study area is large and the terrain is complex, making it difficult to obtain detailed field measurements to validate the results of the analysis, potentially leading to the neglect of regional drivers and response mechanisms. (2) Research on NPP and its response relationship is mainly based on inter-annual changes and does not take into account seasonal or monthly changes within the year, which may ignore seasonal influencing factors.

6. Conclusions

(1) The mean NPP within the South Taihang region is determined to be 307.62 gC m^{-2}, accompanied by an annual growth rate of 3.89 gC m^{-2}. The observed trend exhibits an "N" type variation with ascending altitudes. Notably, regions characterized by elevated and minimal values are situated in the middle and low mountain areas, respectively, particularly in the Jiaozuo-Jiyuan plains.

(2) The region characterized by heightened activity on the plains demonstrated an expansion of approximately fourfold its 2000 level, whereas the active region at higher altitudes experienced a contraction of 36%. The growth of NPP was slowed down by the expansion of the highly active region and aided by the enlargement of the moderately active region.

(3) The climatic conditions displayed an observable trend marked by a gradual increase in temperature and moisture levels. The rates of change in temperature and precipitation were measured at 0.01 °C a^{-1} and 0.96 mm a^{-1}, respectively. Notably, precipitation emerged as a

consistent stimulant for NPP across the entire study area. In contrast, the influence of air temperature was found to be significantly positive only within the medium activity zone and the expanding region.

(4) Precipitation emerges as the predominant factor influencing NPP dynamics across the entire study area. The collective influence of precipitation and human activities in the region, on average, accounts for 79.4% and 19.8%, respectively, of the observed changes in NPP.

Author Contributions

C.M. set the research direction and provided guidance on the research methodology and writing process. C.H. completed the collection and processing of the paper's data, as well as the writing of the paper. T.C. provided financial support. A.G. completed the translation and editing of the article.

Funding

This research was funded by NSFC Regional Innovation Development Joint Fund Key Project (U21A20108), General Project of Natural Science Foundation of Henan Province (242300421365), Support Plan for Technological Innovation Teams in Henan Province's Higher Education Institutions (22IRTSTHN008), General Project for Humanities and Social Sciences in Higher Education Institutions of Henan Province(2024ZZJH147) Co-funded, Research Program of "Double First-class" Creation Project of Surveying and Mapping Science and Technology Discipline (GCCYJ202401).

Institutional Review Board Statement

Not applicable.

Informed Consent Statement

Not applicable.

Data Availability Statement

The NPP data were obtained from the MOD17A3HGF (2000–2020) dataset provided by the US National Aeronautics and Space Administration (NASA), available at (https://ladsweb.modaps.eosdis.nasa.gov/).

The climatological data utilized in this study were obtained from the National Tibetan Plateau Data Center (https://data.tpdc.ac.cn/).

A Prolonged Artificial Night-time light Dataset of China (PANDA) utilized in this study was obtained from the National Tibetan Plateau Scientific Data Center (https://data.tpdc.ac.cn/).

The China Land Cover Dataset (CLCD) utilized in this study was developed by Jie Yang et al. (30 m annual land cover and its dynamics in China from 1990 to 2019 - Zenodo).

The elevation data used in this study are obtained from the NASA Space Shuttle Radar Topographic Mission (SRTM) dataset.

The aforementioned data are accessible free of charge.

Conflicts of Interest

All authors disclosed no relevant relationships.

References

[1] Lieth, H., 1973. Primary production: Terrestrial ecosystems. Human Ecology. 1(4), 303–332. DOI: https://doi.org/10.1007/BF01536729

[2] Chen, X., Zhang, Y., 2023. Impacts of climate, phenology, elevation and their interactions on the net primary productivity of vegetation in Yunnan, China under global warming. Ecological Indicators. 154, 110533. DOI: https://doi.org/10.1016/j.ecolind.2023.110533

[3] Lyu, J., Fu, X., Lu, C., et al., 2023. Quantitative assessment of spatiotemporal dynamics in vegetation NPP, NEP and carbon sink capacity in the Weihe River Basin from 2001 to 2020. Journal of Cleaner Production. 428, 139384. DOI: https://doi.org/10.1016/j.jclepro.2023.139384

[4] Koju, U.A., Zhang, J., Maharjan, S., et al., 2020. Analysis of spatiotemporal dynamics of forest Net Primary Productivity of Nepal during 2000–2015. International Journal of Remote Sensing, 41(11), 4336–4364. DOI: https://doi.org/10.1080/01431161.2020.1717667

[5] Gu, G., Adler, R.F., 2023. Observed variability and trends in global precipitation during 1979–2020. Climate Dynamics. 61(1), 131–150. DOI: https://doi.org/10.1007/s00382-022-06567-9

[6] Chen, S., Ma, M., Wu, S., et al., 2023. Topography intensifies variations in the effect of human activities on forest NPP across altitude and slope gradi-

ents. Environmental Development. 45, 100826. DOI: https://doi.org/10.1016/j.envdev.2023.100826

[7] Xuan, W., Rao, L., 2023, Spatiotemporal dynamics of net primary productivity and its influencing factors in the middle reaches of the Yellow River from 2000 to 2020. Frontiers in Plant Science. 14. DOI: https://doi.org/10.3389/fpls.2023.1043807

[8] Xue, S., Ma, B., Wang, C., et al., 2023. Identifying key landscape pattern indices influencing the NPP: A case study of the upper and middle reaches of the Yellow River. Ecological Modelling. 484, 110457. DOI: https://doi.org/10.1016/j.ecolmodel.2023.110457

[9] Hou, G, Wu, S, Long, W, et al., 2023. Quantitative analysis of the impact of climate change and oasification on changes in net primary productivity variation in mid-Tianshan Mountains from 2001 to 2020. Ecological Indicators. 154, 110820. DOI: https://doi.org/10.1016/j.ecolind.2023.110820

[10] Wang, T., Yang, M., Yan, S., et al., 2021. Effects of temperature and precipitation on spatiotemporal variations of net primary productivity in the Qinling Mountains, China. Polish Journal of Environmental Studies. 30(1), 409–422. DOI: https://doi.org/10.15244/pjoes/122839

[11] Ma, B., Jing, J., Liu, B., et al., 2022. Quantitative assessment of the relative contributions of climate change and human activities to NPP changes in the Southwest Karst area of China. Environmental Science and Pollution Research. 29(53), 80597–80611. DOI: https://doi.org/10.1007/s11356-022-21433-1

[12] Zhang, H., Sun, R., Peng, D., et al., 2021. Spatiotemporal dynamics of net primary productivity in China's urban lands during 1982–2015. Remote Sensing. 13, 400. DOI: https://doi.org/10.3390/rs13030400

[13] Azhdari, Z., Sardooi, E.R., Bazrafshan, O., et al., 2020. Impact of climate change on net primary production (NPP) in south Iran. Environmental monitoring and assessment. 192(6), 409. DOI: https://doi.org/10.1007/s10661-020-08389-w

[14] Zarei, A., Chemura, A., Gleixner, S., et al., 2021. Evaluating the grassland NPP dynamics in response to climate change in Tanzania. Ecological Indicators. 125, 107600. DOI: https://doi.org/10.1016/j.ecolind.2021.107600

[15] Ivan, K., Holobaca, I.-H., Benedek, J., et al., 2020. Potential of night-time lights to measure regional inequality. Remote Sensing. 12(1), 33. DOI: https://doi.org/10.3390/rs12010033

[16] Bagan, H., Borjigin, H., Yamagata, Y., 2018. Assessing nighttime lights for mapping the urban areas of 50 cities across the globe. Environment and Planning B: Urban Analytics and City Science. 46, 239980831775292. DOI: http://dx.doi.org/10.1177/2399808317752926

[17] Ghosh, T., Anderson, S.J., Elvidge, C.D., et al., 2013. Using nighttime satellite imagery as a proxy measure of human well-being. Sustainability. 5(12), 4988–5019. DOI: https://doi.org/10.3390/su5124988

[18] Peng, S., 2020. 1-km monthly mean temperature dataset for china (1901–2022). DOI: https://dx.doi.org/10.11888/Meteoro.tpdc.270961

[19] Peng, S., 2020. 1-km monthly precipitation dataset for China (1901–2022). DOI: https://dx.doi.org/10.5281/zenodo.3185722

[20] Zhang, L., Chen, B., Fu, H., et al., 2021. A Prolonged Artificial Nighttime-light Dataset of China (1984–2020). DOI: https://dx.doi.org/10.11888/Socioeco.tpdc.271202

[21] Yang, J., Huang, X., 2021. The 30 m annual land cover datasets and its dynamics in China from 1990 to 2020. DOI: https://doi.org/10.5281/zenodo.5210928

[22] Ma, T., Zhou, Y., Zhou, C., et al., 2015. Night-time light derived estimation of spatio-temporal characteristics of urbanization dynamics using DMSP/OLS satellite data. Remote Sensing of Environment. 158, 453–464. DOI: https://doi.org/10.1016/j.rse.2014.11.022

[23] Li, Y., Qin, Y., 2019. The response of Net Primary Production to climate change: A case study in the 400 mm annual precipitation fluctuation zone in China. International Journal of Environmental Research and Public Health. 16(9), 1497. DOI: https://doi.org/10.3390/ijerph16091497

[24] Tang, R., Zhao, X., Zhou, T., et al., 2018. Assessing the impacts of urbanization on albedo in Jing-Jin-Ji region of China. Remote Sensing. 10(7). DOI: https://doi.org/10.3390/rs10071096

[25] Forzieri, G., Alkama, R., Miralles, D.G., et al., 2017. Satellites reveal contrasting responses of regional climate to the widespread greening of Earth. Science. 356(6343), 1180–1184. DOI: https://doi.org/10.1126/science.aal1727

[26] Zhao, L., Chen, Y., Wang, X., et al., 2022. Spatiotemporal changes in net primary productivity before and after the development of unused land in the hilly areas of Hebei, China. PlOS ONE. 17(6), e0270010. DOI: https://doi.org/10.1371/journal.pone.0270010

[27] Yang, A., Zhang, H., Yang, X., et al., 2022. Quantitative analysis of the impact of climate change and human activities on vegetation NPP in the Qilian Mountain. Human and Ecological Risk Assessment: An International Journal. 29, 202–221. DOI: https://doi.org/10.1080/10807039.2022.2152774

[28] Xu, Y., Xu, X., Tang, Q., 2016. Human activity intensity of land surface: Concept, methods and application in China. Journal of Geographical Sciences. 26, 1349–1361. DOI: https://doi.org/10.1007/s11442-016-1331-y

[29] Linger, E., Hogan, J.A., Cao, M., et al., 2020. Precipitation influences on the net primary productivity of a tropical seasonal rainforest in Southwest China: A 9-year case study. Forest Ecology and Management. 467, 118153. DOI: https://doi.org/10.1016/j.foreco.2020.

118153

[30] Wang, X.C., Wang, S.D., Zhang, H.B., 2013, Spatiotemporal pattern of vegetation net primary productivity in Henan Province of China based on MOD17A3. Chinese Journal of Ecology. 32, 2797–2805. DOI: https://doi.org/10.13292/j.1000-4890.2013.0314

[31] Li, J., Liu, Y., Cao, M., et al., 2015. Space-time characteristics of vegetation cover and distribution: Case of the Henan Province in China. Sustainability. 7, 11967–11979. DOI: https://doi.org/10.3390/su70911967

[32] Luo, Y., Zhou, M., Jin, S., et al., 2023. Changes in phylogenetic structure and species composition of woody plant communities across an elevational gradient in the southern Taihang Mountains, China. Global Ecology and Conservation. 42, e02412. DOI: https://doi.org/10.1016/j.gecco.2023.e02412

[33] Li, T., Guo, Z., Chao, M., 2022. Dynamic characteristics of urbanization based on nighttime light data in China's "plain–mountain transition zone". International Journal of Environmental Research and Public Health. 19, 9230. DOI: https://doi.org/10.3390/ijerph19159230

[34] Wang, Q., Liu, K., Ni, X., et al., 2023. Extreme climate change and contemporary analogs for cities in mainland China in a 2.0 °C warmer climate. Climate Services. 30, 100348. DOI: https://doi.org/10.1016/j.cliser.2023.100348